Comparison of Q3s ATD Biomechanical Responses to Pediatric Volunteers

M. Ita[1,2], T. Seacrist[3], E. Dahle[4], J. Bolte IV[1,5], Y. Kang[1,5]

1. Injury Biomechanics Research Center, The Ohio State University
2. Department of Biomedical Engineering, The Ohio State University
3. Center for Injury Research and Prevention, Children's Hospital of Philadelphia
4. Evenflo Company, Inc.
5. Division of Anatomy, The Ohio State University

ABSTRACT

The biofidelity of pediatric ATDs continues to be evaluated with scaled-down adult data, a methodology that requires inaccurate assumptions about the likeness of biomechanical properties of children and adults. Recently, evaluation of pediatric ATDs by comparison of pediatric volunteer (PV) data has been shown to be a valuable and practical alternative to the use of scaled adult data. This study utilized existing PV data to evaluate a 3 year-old side impact ATD, the Q3s. While ATDs have been compared to volunteer responses in frontal impacts, this study is the first to extend ATD-PV comparison methods to the Q3s ATD, and among the first to extend these methods to side impacts.

Previously conducted experiments were replicated in order to make a direct comparison between the Q3s and PVs. PV data were used from 4-7 year-olds (shoulder tests, n=14) and 6-8 year-olds (sled tests, n=7). Force-deflection data were captured during quasi-static shoulder tests through manual displacement of the shoulder joint. Resulting shoulder stiffness was compared between the Q3s and PVs. Low-speed far-side sled tests were conducted with the Q3s at lateral (90°) and oblique (60°) impacts. Primary outcomes of interest included 1) lateral displacement of the torso, 2) torso rollout angle, and 3) kinematic trajectories of the head and neck.

The Q3s exhibited shoulder stiffness values at least 32 N/mm greater than the PVs for all conditions. In low-speed sled tests, overall the Q3s and PV trajectories were of similar shape, although Q3s head kinematics displayed rigid body motion followed by independent lateral bending of the head, suggesting cervical and thoracic spine rigidity compared to PVs. This study provides a dataset comparing the biomechanical responses for the Q3s ATD and pediatric volunteers at low severity impacts. Even at low severity impacts, we can identify biomechanical response differences between children and the Q3s which can contribute to design improvements leading to more biofidelic pediatric ATDs.

INTRODUCTION

Side impacts have been identified as a priority in the area of child occupant protection, as side impacts have been studied very little relative to frontal impacts even though higher fatality rates have been observed in side relative to frontal impacts (Arbogast and Durbin 2013; Starnes and Eigen 2002; Viano and Parenteau 2008). Until recently, however, the lack of an adequately biofidelic pediatric side impact anthropomorphic test device (ATD) has been a major limitation in the ability to accurately capture and assess occupant behavior and interaction with restraint systems in side impacts. The 3 year-old targeted Q3s ATD, part of the Q-series ATD family, is one of the first side impact specific pediatric ATDs that is emerging as a tool to fill this need.

Since the introduction of pediatric ATDs into the industry, biofidelity and robustness have been evaluated using scaled-down cadaveric adult data. Using scaled adult data for pediatric ATD evaluation requires many assumptions about the biomechanical, anthropomorphic, and injury responses of children relative to adults. Numerous studies have reported the effect of age on material and structural properties of the human anatomy, and the implications that age effects have on injury response and mechanism (Burdi et al. 1969; McCray et al. 2007; Starnes & Eigen 2002). While methodologies originally developed to normalize and scale adult data have been modified to attempt to accommodate pediatric ATDs (Irwin & Mertz 1997; Melvin 1995; van Ratingen et al. 1997; Wolanin et al. 1982), these modifications do not adequately account for differences between children and adults.

Limited studies have been conducted that compare pediatric ATDs and child-size post-mortem human subjects (PMHS) in crash-like scenarios which demonstrate non-biofidelic responses of pediatric ATDs (Ash et al. 2009; Lopez-Valdes et al. 2009; Sherwood et al. 2002). Recently, several studies have taken advantage of pediatric volunteer (PV) data to evaluate ATD biofidelity (Seacrist et al. 2010, 2012, 2013, 2014). PV data is more readily attainable compared to pediatric PMHS, and is emerging as a valuable tool for evaluation of ATD whole body kinematic responses.

The evaluation of Q3s biofidelity is of growing importance as side impact requirements are incorporated into CRS regulation (Martin, 2013). The study presented here utilizes PV data to evaluate the shoulder and overall kinematics of the Q3s ATD. While ATDs have been compared to volunteer responses for frontal impacts, this study is the first to extend ATD-PV comparison methods to the Q3s ATD, and among the first to extend these methods to side impacts.

METHODS

Previously conducted experiments were replicated in order to make a direct comparison between the Q3s and PVs. The two experiments, quasi-static shoulder experiments and low-speed far-side sled tests, are explained in the following sections. Detailed methods as described in the original publications can be found in Suntay et al. (2011) and Arbogast et al. (2012).

Shoulder Stiffness Experiments (Suntay et al. 2011.)

Setup and instrumentation: Force measurements were captured using a custom force applicator with an attached load cell (Honeywell Model 31 Mid-Range Precision Miniature). The frame of the force applicator allowed for rotational movement such that the applicator could be positioned for a medial loading direction (0°) or a posteromedial loading direction (30°). A shoulder-height wall was positioned on the non-loading side of the Q3s to prevent lateral excursion and subject "tilt." Displacement measurements were captured using an 8-camera, 100 Hz Vicon motion analysis system (Vicon Motion Systems, Oxford, UK). Reflective markers were placed on the Q3s right acromion, left acromion, and sternum.

The Q3s was positioned on the testing bench (Figure 1) such that the ATD spine aligned with the edge of the bench, and the force applicator load cell aligned with the Q3s shoulder joint. Each trial consisted of manual force application to displace the shoulder for 5 to 10 seconds. Three trials were performed on the Q3s right shoulder for both the medial and posteromedial loading directions.

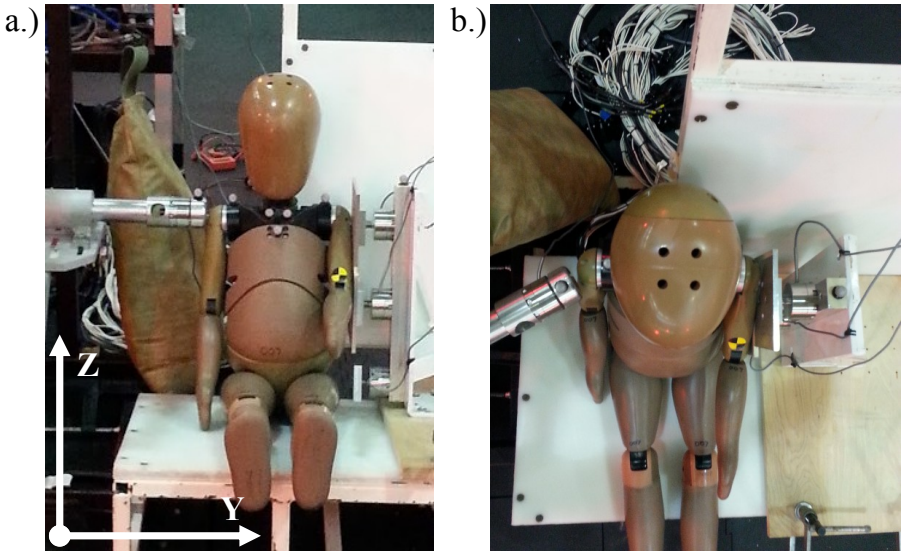

Figure 1: Q3s positioned for a.) a medial loading trial and b.) a posteromedial loading trial.

Data Reduction and Analysis: Motion capture data were acquired at 100 Hz and processed using Vicon Nexus software. Force and linear potentiometer data were captured at 1,000 Hz and filtered with a low-pass butterworth filter at 100 Hz. Shoulder deflection was calculated from both the right acromion to sternum (half-thoracic) and from the right acromion to the left acromion (full-thoracic) in the xy-plane. Data were truncated at the point where subject tilt exceeded 4° from initial position or at the maximum force achieved during the trial (Bolte et al. 2003; Suntay et al. 2011).

Since shoulder stiffness values were calculated as the slope of the resulting force-deflection curves, a viably linear portion of the curve was defined as the middle 20-80% of the curve based off of the peak force measurement. For the PV analysis, force-deflection data of individual trials were omitted from the analyses if the output force-deflection curves either 1) displayed exclusively negative deflection or 2) were deemed to contain no viably linear portion. In order to plot Q3s against PV shoulder response, individual force-deflection curves were created for each subject by interpolating repeated subject trials onto common values of deflection (Suntay et al. 2011). Deflection measurements less than 2 mm were consistently observed in PV force-deflection curves in the medial loading condition. These data were not originally published with the pediatric data because a deflection less than 2 mm could be attributed to only skin deflection, as described by Suntay (Suntay et al. 2011). Thus, only posteromedial loading data are presented here for comparison.

Low-Speed Far-Side Sled Experiments (Arbogast et al. 2012)

Setup and instrumentation: Low-speed far-side sled tests were conducted with a pneumatically actuated and hydraulically controlled low-speed crash sled (Figure 2a) which could be rotated to allow for sled pulses applied to various directions relative to the sled occupant. In this study, sled pulses were applied to mimic a purely lateral (90°) and an oblique impact (60°). For both PV and Q3s sled tests, the average sled pulse acceleration and rise time were approximately 1.8 g, 59.7 ms and 1.9 g, 54.4 ms for lateral and oblique trials, respectively.

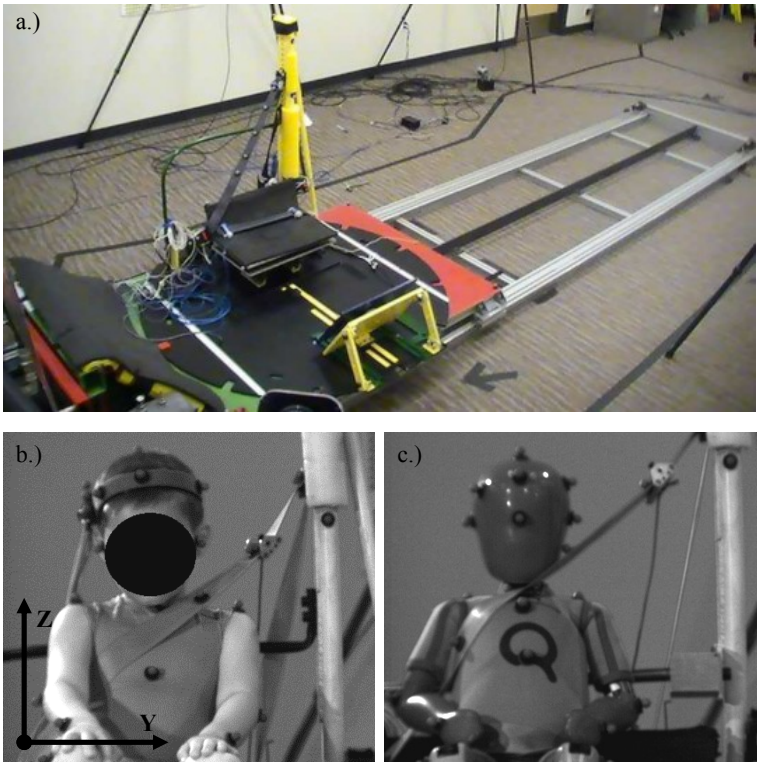

Figure 2: The low speed crash sled (a.), and a 6 year-old pediatric volunteer (b.) and the Q3s (c.) in the sled at initial position.

Reaction forces were acquired from various sled and seat instrumentation channels, including a sled accelerometer, a shoulder belt load cell, left and right lap belt load cells, and 6-axis seat pan and foot rest load cells. Q3s instrumentation data were acquired for head acceleration and angular rotation in the x, y, and z-directions, T1 acceleration in the y-direction, upper spine acceleration in the x, y, and z-directions, and a 6-axis load cell in the upper neck. Reflective markers placed on the Q3s in the orientation previously used for pediatric subjects were tracked with a 3D motion analysis system (Model Eagle 4, Motion Analysis Corporation, Santa Rosa, CA). This included markers on the head, torso, spine, and extremities. Reflective markers were also placed on the seat pan and sled.

The Q3s was positioned as described by Arbogast et al. (2012). Positioning included setting the initial torso and knee flexion angles to 110° through adjustments to the foot rest on which the Q3s feet rested. To accommodate the decreased seated height of the Q3s relative to volunteers, the back rest was adjusted such that it fell between T4 and T8 to achieve the same torso angle relative to ground as volunteer subjects. The shoulder and lap belt angles, defined as the angle made with the horizontal, were set to 55°. The height of the shoulder belt D-Ring was

adjusted to achieve the 55° shoulder belt angle. Surrogates were restrained with an automotive three-point seat belt (Takata Corp., Tokyo, Japan). An image of a 6 year-old volunteer and the Q3s at initial position can be seen in Figure 2b and 2c, respectively. For this study, two trials were conducted for each subject at either the lateral or oblique impact angle (the Q3s was tested in both).

Data Reduction and Analysis: Motion capture data were acquired at 100 Hz and analyzed using Cortex 2.6 software (Motion Analysis, Inc.). On-board accelerometer and load cell data, as well as Q3s instrumentation channels, were captured at 10,000 Hz with a built-in anti-aliasing filter at 4,300 Hz. Sled and Q3s instrumentation signals were filtered at SAE J211 standards at SAE channel frequency class (CFC) 60. ARS signals were filtered at CFC 1000.

For motion capture data, a reflective marker at the right rear of the seat pan was designated as the origin for the local sled coordinate system. Primary outcomes of interest for this study included: 1) lateral displacement of the torso, 2) torso rollout angle projected onto the coronal and transverse planes, and 3) trajectories over time for markers on the top of the head, C4, and T1. Lateral displacement of the torso was calculated using movement of the suprasternal notch (SSN) marker (Arbogast et al. 2012). Torso rollout angle was calculated as the projected angle made between the line connecting the SSN and xiphoid process and the line connecting markers on the shoulder belt (Arbogast et al. 2012). Maximum excursions were calculated for marker trajectories of interest as the change from initial position to maximum excursion. Time at maximum was also recorded for all outcomes. Average trajectories, excursions, torso displacement, and torso rollout angles were calculated for lateral and oblique trials for the PVs and compared to the Q3s. Peaks and time at peak were calculated and averaged for the PV group and a 95% confidence interval (CI) for the PVs was calculated for each outcome using JMP software (JMP 10 SAS, Cary, NC).

Length Scaling: In order to compare the kinematics of the PV group to the Q3s, PV kinematic data were length scaled based on dimensional analysis (Ash et al. 2009.; Irwin et al. 2002). Kinematic trajectories and torso displacement were scaled using a scaling factor (λ_L) defined as the ratio between the seated height of the Q3s (L_{Q3s}) and the seated height of the PV (L_{PV}), as shown in Eq. (1).

$$\lambda_L = \frac{L_{Q3s}}{L_{PV}} \qquad (1)$$

Scaling was deemed necessary because although the smallest age-group of available PV data were used (6-8 years-old), the PVs were not size-matched to the Q3s. As only kinematic data are presented in this study, no other scaling factors were required.

Pediatric Volunteers

PV data for shoulder stiffness experiments were used from 14 subjects ages 4 to 7 years-old (Suntay et al. 2011). Force-displacement data were collected in both the muscle tensed and muscle relaxed condition for every volunteer. PV data for the low-speed far-side sled tests were used from 7 subjects ages 6 to 8 years-old (Seacrist et al. 2014). PV subject and test information for both shoulder and sled tests can be found in Tables 1 and 2, respectively.

Table 1: PV anthropometric measurements for shoulder experiments

Subject No.	Sex	Age	Mass	Seated Height
		years	kg	cm
1	F	6	18.6	63.9
2	F	5	19.5	61.0
3	F	4	21.3	60.5
4	M	6	20.9	63.5
5	F	6	24.9	62.0
6	M	4	20.9	57.0
7	M	6	23.6	60.5
8	F	4	18.8	54.5
9	M	7	24.0	68.0
10	M	6	19.5	64.0
11	M	5	20.4	66.0
12	F	6	25.4	68.5
13	F	7	23.1	67.0
14	M	5	20.0	65.0

Table 2: PV anthropometric subject and test information for sled tests

Subject No.	Test Condition	Sex	Age	Mass	Seated Height
	deg		years	kg	cm
PV Lat 1	90	M	8	36.7	73.5
PV Lat 2	90	M	6	28.8	68.5
PV Lat 3	90	M	7	32.7	67.0
PV Lat 4	90	M	7	29.7	69.8
PV Obl 1	60	M	8	28.1	68.5
PV Obl 2	60	M	7	27.4	64.8
PV Obl 3	60	M	6	20.2	66.0

RESULTS

Shoulder Stiffness Results

Force-deflection curves for both the Q3s and the PV group (Figure 3) were plotted according to both 1) deflection calculation (full-thoracic or half-thoracic) and 2) PV test condition (muscles relaxed or tensed). The calculated Q3s shoulder stiffness values, as seen in Figure 3, were much higher than any of the stiffness values (relaxed and tensed) exhibited by the PVs.

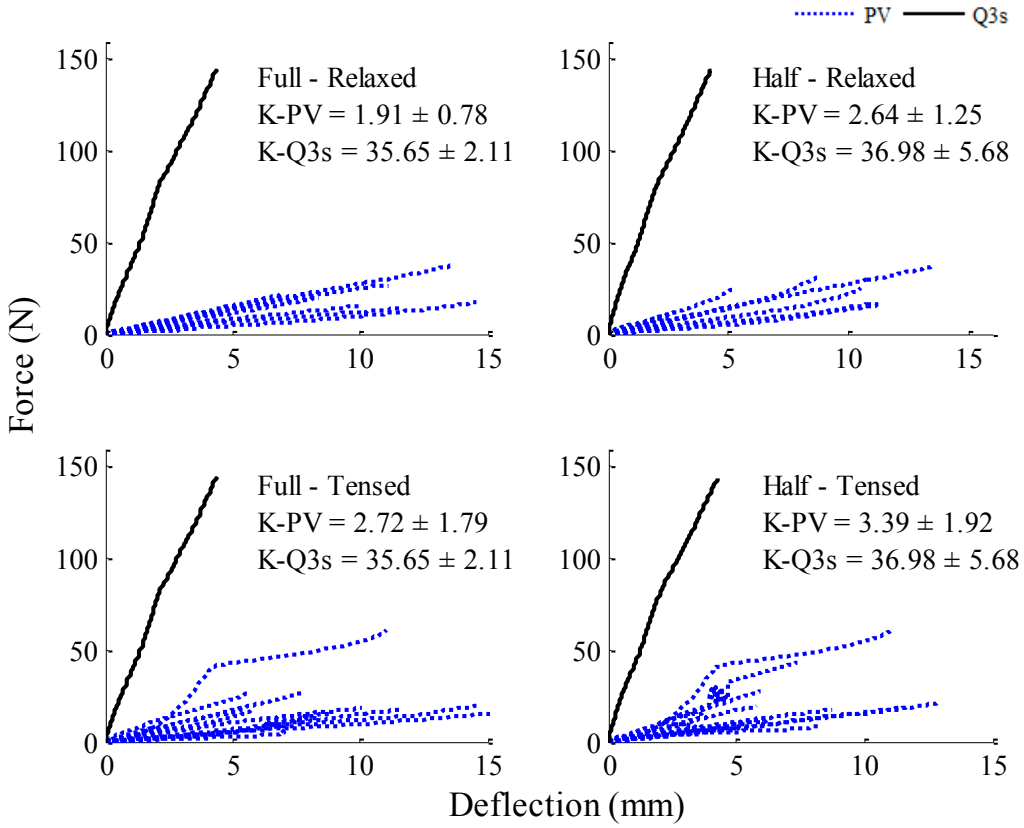

Figure 3: Force-deflection curves plotted for the Q3s and PV group for the posteromedial loading direction. Each PV curve represents the mean response from one pediatric subject. Q3s force-deflection curve is plotted against the PV mean curves for both the full-thoracic (Full) and half-thoracic (Half) deflection calculations in both the relaxed and tensed test conditions. Stiffness values (K) are listed as mean ± one standard deviation in N/mm.

Low-Speed Far-Side Sled Test Results

Plots presented for sled test results show one mean curve per subject for simplicity (two trials were conducted). Although one mean curve was plotted per subject, peak and standard deviation for outcome maximums (Tables 3 and 4) were calculated on a trial-by-trial basis so as not to introduce skewing of extreme peaks by curve averaging. Images of the Q3s and a 6 year-old volunteer can be seen in Figure 4 at initial position, 200 ms after impact, and 400 ms after impact.

Torso Displacement: Comparison of torso displacement, as represented by lateral displacement of the suprasternal notch (SSN) marker, can be seen between the Q3s and PVs in Figure 5. Peak SSN displacement values and time at peak for the Q3s and PVs, as well as a 95% CI for the PVs, are located in Table 3. Quantitatively, the Q3s exhibited significantly delayed (Q3s peaks not within 95% CI) times to peak torso displacement for both lateral and oblique trials. Qualitatively, however, a delay in time to peak for lateral and oblique trials is difficult to discern from the plots (Figure 5) and is likely not a meaningful difference. While torso displacement was larger for the Q3s than the PVs in lateral trials, torso displacement was not significantly different (Q3s peaks did lie within 95% CI) for oblique trials.

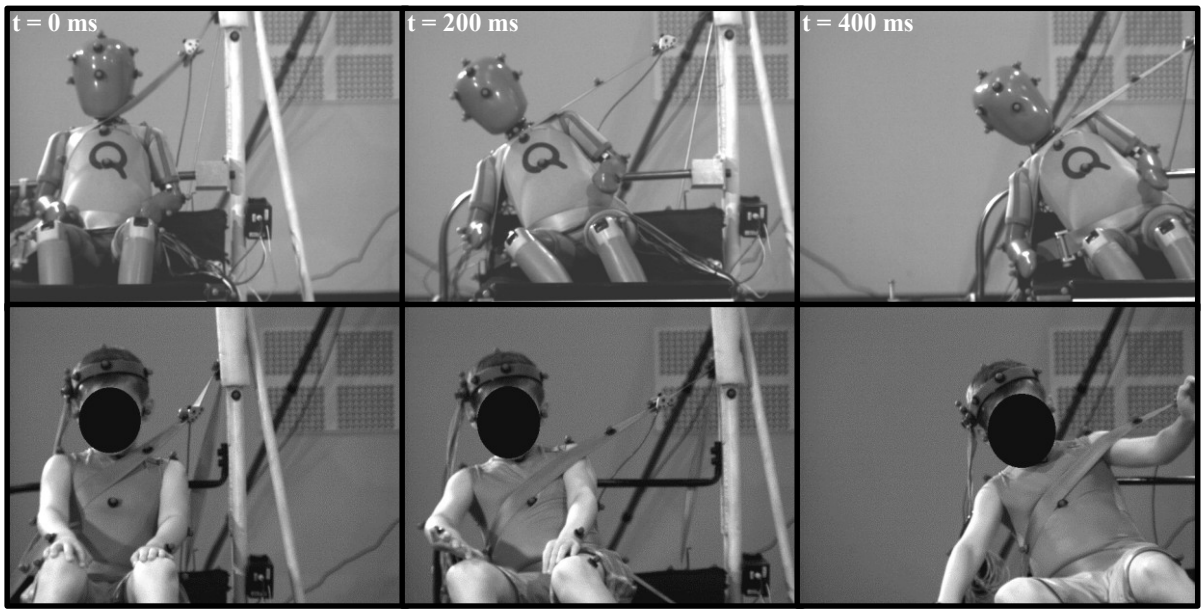

Figure 4: Images of the Q3s (top panel) and a 6 year-old volunteer (bottom panel) at initial position (time = 0 ms), at time = 200 ms, and at the approximate time of maximum head lateral excursion (time = 400 ms) during a lateral impact trial.

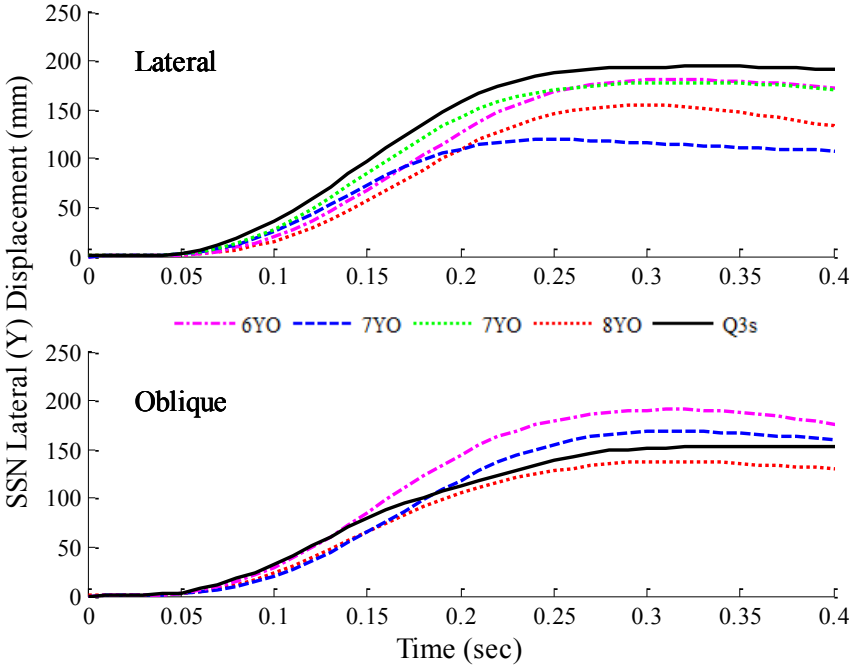

Figure 5: Lateral displacement (y-direction) of the SSN marker. Q3s plotted against PV mean curves for lateral and oblique trials. Legend indicates age of PV per curve, but like lines across lateral and oblique trials do not indicate the same subject.

Table 3: Peak and time at peak for SSN Y-displacement and torso rollout angles; shaded cells indicate a significant difference between the Q3s and PVs at significance level of .05

			Q3s (Mean)	PV (Mean±SD)	PV 95% CI
Lateral	SSN Y-displacement	Peak (mm)	194.6	164.3 ± 26.6	139.7 - 188.9
		Time (msec)	34.0	29.6 ± 2.8	27.0 - 32.2
	Transverse Rollout Angle	Peak (deg)	45.4	42.7 ± 10.2	32.0 - 53.4
		Time (msec)	39.0	32.0 ± 2.2	29.7 - 34.3
	Coronal Rollout Angle	Peak (deg)	49.2	35.7 ± 12.4	22.7 - 48.8
		Time (msec)	33.5	31.7 ± 2.0	29.6 - 33.7
Oblique	SSN Y-displacement	Peak (mm)	153.3	166.2 ± 24.5	140.4 - 191.9
		Time (msec)	37.0	31.8 ± 1.7	30.0 - 33.6
	Transverse Rollout Angle	Peak (deg)	45.9	37.9 ± 10.8	10.9 - 64.9
		Time (msec)	33.0	34.7 ± 6.3	18.9 - 50.4
	Coronal Rollout Angle	Peak (deg)	42.8	39.5 ± 2.3	33.7 - 45.4
		Time (msec)	38.5	34.3 ± 4.9	22.1 - 46.6

Rollout Angle: Torso rollout angle was projected onto both the transverse (x-y) and coronal (y-z) planes (Figure 6). Peak rollout angles and times at peak for the Q3s and PVs, as well as a 95% CI for the PVs, are located in Table 3. In the lateral trials, the Q3s exhibited a similar peak but delayed rollout as compared to the PVs in the transverse plane. In the coronal plane, the Q3s exhibited a similar time to peak but greater rollout angle. In the oblique trials, the Q3s did not exhibit differences from the PVs in terms of peak or time at peak in either plane projection.

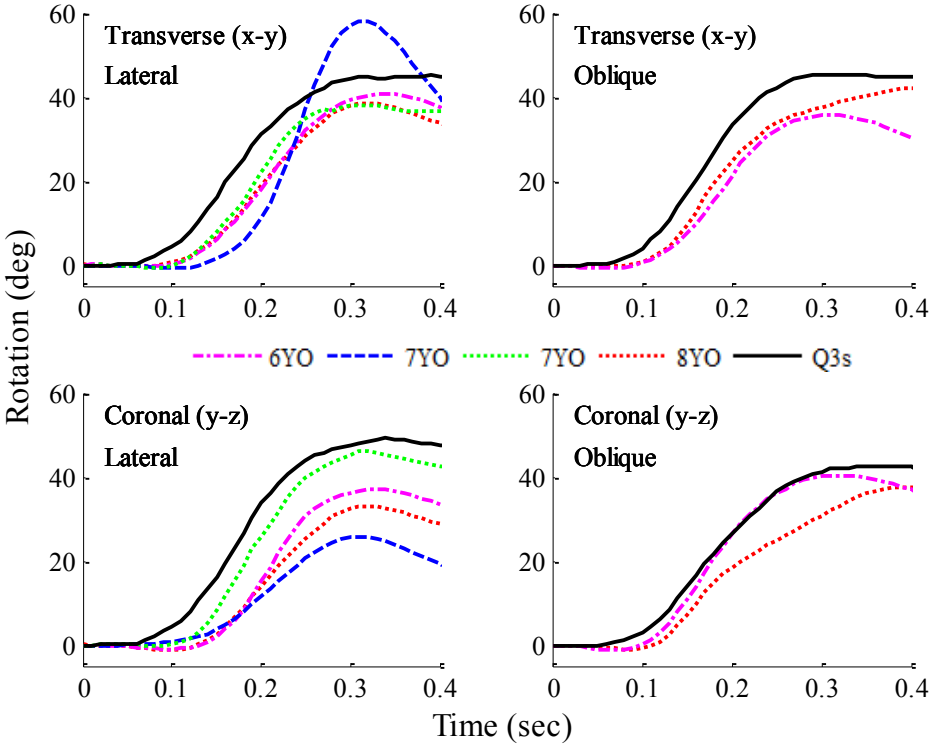

Figure 6: Torso rollout angle projected onto the transverse (x-y) plane (top) and the coronal (y-z) plane (bottom). Q3s plotted against PV mean curves for lateral and oblique trials. Legend indicates age of PV per curve, but like lines across lateral and oblique trials do not indicate the same subject.

Kinematic Trajectories of the Head and Neck: Trajectories of the head top (HT), C4, and T1 markers were plotted in the coronal (y-z) plane as shown in Figure 7. Maximum excursion from initial position and time at maximum for the Q3s and PVs, as well as a 95% CI for the PVs, are located in Table 4.

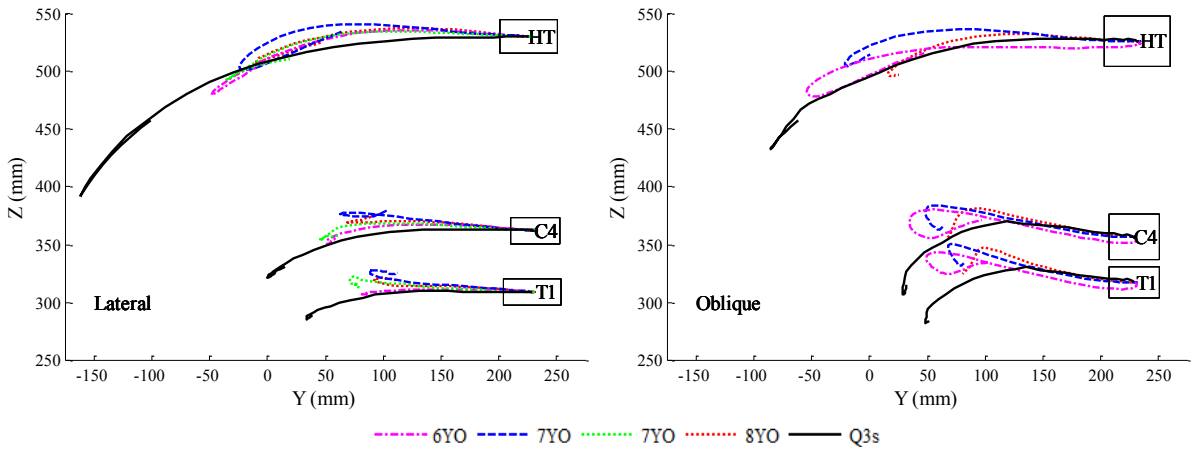

Figure 7: Kinematic trajectories of markers on the top of the head (HT), C4, and T1 in the coronal (y-z) plane. Q3s plotted against PV mean curves for lateral and oblique trials. Trajectories were adjusted to begin at the average initial (y,z) point. Rectangles indicate one standard deviation of initial (y,z) starting point. Legend indicates age of PV per curve, but like lines across lateral and oblique trials do not indicate the same subject.

DISCUSSION

This study aimed to evaluate biomechanical responses of the Q3s ATD against the youngest PV data available in side impact loading conditions. Stiffness was calculated for the Q3s and PVs in order to evaluate structural properties of the Q3s shoulder. Low-speed far-side sled test results highlighted differences in kinematic movement during lateral and oblique loadings.

Pediatric Comparison Group

In choosing a PV group for Q3s comparison, the 4-8 year-old group (4-7 year-old shoulder tests, 6-8 year-old sled tests) was chosen because it was the youngest data set available and therefore closest to the target age of the Q3s. While maturation changes existing between 3 year-old and 4-8 year-old children should not be ignored in Q3s-PV comparisons, it should be noted that maturation changes between these age groups will be less drastic than those observed between a 3 year-old and 18 year-old, or between a 3 year-old and adult PMHS, and so on. It is believed that a comparison to younger PVs will help mitigate implications of the assumptions between ATD target age and comparison group often problematic in scaling methodologies. Despite an age gap, 4-8 year old PVs provide a robust data set for Q3s evaluation. For example, cervical spine range of motion (ROM) measurements were compared between children 3-5 years-old and 6-8 years-old (Arbogast et al. 2007). ROM measures that did not show a difference with age included right and left lateral bending. These findings partially help to

validate conclusions drawn from side impact kinematics between the target-aged 3 year-old Q3s and the 4-8 year-old PVs.

Table 4: Maximum excursion and time at maximum for ΔY and ΔZ trajectories; shaded cells indicate a significant difference between the Q3s and PVs at significance level of .05

			Q3s (Mean)	PV (Mean±SD)	PV 95% CI
Lateral	HT	Max (mm)	-389	-258 ± 21	-277 - -239
	ΔY	Time (msec)	32	32 ± 2	31 - 34
	HT	Max (mm)	-140	-37 ± 12	-48 - -25
	ΔZ	Time (msec)	32	33 ± 2	31 - 35
	C4	Max (mm)	-231	-177 ± 18	-193 - -160
	ΔY	Time (msec)	34	30 ± 5	26 - 35
	C4	Max (mm)	-41	0 ± 15	-14 - 14
	ΔZ	Time (msec)	35	38 ± 6	32 - 43
	T1	Max (mm)	-196	-149 ± 15	-163 - -135
	ΔY	Time (msec)	34	29 ± 6	24 - 34
	T1	Max (mm)	-24	9 ± 9	1 - 18
	ΔZ	Time (msec)	36	32 ± 8	25 - 39
Oblique	HT	Max (mm)	-319	-251 ± 33	-285 - -217
	ΔY	Time (msec)	36	34 ± 1	32 - 35
	HT	Max (mm)	-96	-34 ± 14	-48 - -20
	ΔZ	Time (msec)	36	37 ± 3	33 - 40
	C4	Max (mm)	-200	-179 ± 15	-195 - -163
	ΔY	Time (msec)	32	33 ± 5	27 - 38
	C4	Max (mm)	-50	21 ± 19	0 - 41
	ΔZ	Time (msec)	35	27 ± 9	18 - 36
	T1	Max (mm)	-181	-163 ± 15	-179 - -148
	ΔY	Time (msec)	30	34 ± 7	26 - 41
	T1	Max (mm)	-36	31 ± 8	22 - 40
	ΔZ	Time (msec)	34	25 ± 2	23 - 28

Shoulder Stiffness

The increased shoulder stiffness of the Q3s relative to the PVs is consistent with results of dynamic testing of the Q3s shoulder conducted by NHTSA, where the Q3s shoulder exhibited high shoulder stiffness against lateral and oblique corridors (Bolte et al. 2003; Irwin et al. 2002; Martin 2013). While the argument exists that a more compliant shoulder joint would compromise durability of the Q3s as a testing tool, a high-stiffness shoulder could have implications on the response of the thorax and head. In side impacts, the shoulder of a pediatric occupant often interacts first with an intruding vehicular structure or restraint system (Suntay et al., 2011). Shoulder deflection due to medial loading results in initial impact load distribution to the spinal column and head, so a high-stiffness shoulder complex may affect loads seen by the head and thorax (Thollon et al. 2001). This is extremely relevant to pediatric occupants, as children in side impacts compared to frontal are significantly more likely to suffer severe injuries to the head and thorax (Brown et al. 2006).

Kinematic Differences

In the lateral trials, the combined increased torso displacement and coronal plane trajectories demonstrated that the Q3s experienced an overall total body lateral excursion greater than the PVs. Increased torso rollout in the coronal plane, along with increased excursions of the HT-C4-T1 complex, are consistent with increased lateral bending observed in the Q3s. Especially large ΔY and ΔZ were observed for the Q3s HT marker. A qualitative analysis of the lateral trajectories in Figure 7 and the images in Figure 4 indicates rigid body motion of the Q3s between the HT, C4, and T1. Toward the end of the trajectory, however, the Q3s HT marker appears to have achieved greater lateral bending than the C4 and T1 markers. Rigid body motion followed by increased lateral bending of the head (resembling a “head snap” motion) was consistent with high speed videos of the Q3s. In contrast, the PVs did not exhibit this rigid body motion to the same extent as the Q3s, as near the end of the trajectory the C4 and T1 markers deviated upwards from initial position, toward HT.

Spine rigidity of both the cervical and thoracic spines likely contributed to observed kinematic differences. Kinematic differences between pediatric ATDs and PVs (Seacrist et al. 2010, 2012) or PMHS (Ash et al. 2009; Sherwood et al. 2002) have previously been attributed to non-biofidelic motion of the ATD thoracic spine in frontal impacts. Little data, however, is available in terms of PV-ATD comparison in side impact or with side impact ATDs. Conclusions drawn regarding an overly rigid cervical and/or thoracic spine in the Q3s should be considered with the understanding that kinematic differences may not hold true for higher severity impacts.

Exact replication of the low-speed far-side sled tests was necessary in order to make a direct comparison between the Q3s and PVs. A limitation exists here, however, in that the setup utilized a three-point seat belt, while a 3 year-old occupant would (ideally) be constrained to a CRS. Additionally, although the initial position angles described in Methods were matched in the Q3s tests to those tests conducted with volunteers, there were differences in the fit of the three-point seat belt, as seen in Figures 2 and 4. Thus, there are concerns about the equivalence of the loading environment between the Q3s and PVs due to seat belt slip up the Q3s torso (as seen in Figure 4). This limitation should be considered along with differences observed between the Q3s and PVs. While the sled test environment was not age specific to the Q3s, it is valuable in that it provided a dataset of unconstrained movement ideal for ATD-PV comparison.

CONCLUSIONS

This study aimed to evaluate the Q3s shoulder joint and overall kinematics by comparison to pediatric volunteer data. This was one of the first studies to utilize ATD-pediatric volunteer methods in side impacts and the first study to use these methods to evaluate the Q3s. These results provide an important step toward ATD pediatric biofidelity evaluation by comparison to volunteer data at low severity impacts. Even at low severity impacts, we can identify biomechanical response differences between children and the Q3s which can contribute to design improvements leading to more biofidelic pediatric ATDs.

ACKNOWLEDGEMENTS

The authors would like to acknowledge the National Science Foundation (NSF) Center for Child Injury Prevention Studies at the Children's Hospital of Philadelphia (CHOP) and the Ohio State University (OSU) for sponsoring this study and its Industry Advisory Board (IAB) members for their support, valuable input and advice. The views presented are those of the authors and not necessarily the views of CHOP, OSU, the NSF, or the IAB members. The authors would like to acknowledge NHTSA-VRTC for use of the Q3s ATD. Additional acknowledgements go out to CHOP for both their help in conducting the sled tests and sharing data used for comparison.

REFERENCES

Arbogast KB, Gholve PA, Friedman JE, Maltese MR, Tomasello MF, Dormans JP. Normal cervical spine range of motion in children 3–12 years old. *Spine.* 2007;32(10):309–315.

Arbogast KB, Mathews EA, Seacrist T, Maltese MR, Hammond R, Balasubramanian S, Kent RW, Tanji H, St. Lawrence S, Higuchi K. The effect of pretensioning and age on torso rollout in restrained human volunteers in far-side lateral and oblique loading. *Stapp Car Crash J.* 2012;56:443–467.

Arbogast KB, Durbin DR. Epidemiology of child motor vehicle crash injuries and fatalities. In: Crandall JR, Myers BS, Meaney DF, Zellers Schmidtke S, eds. *Pediatric Injury Biomechanics: Archive & Textbook*. New York, NY: Springer; 2013:33–86.

Ash J, Abdelilah Y, Crandall J, Parent D, Sherwood C, Kallieris D. Comparison of anthropomorphic test dummies with a pediatric cadaver restrained by a three-point belt in frontal sled tests. Paper presented at: 21st International Technical Conference on the Enhanced Safety of Vehicles; June 15-18, 2009; Stuttgart, Germany.

Bolte IV JH, Hines MH, Herriott RG, McFadden JD, Donnelly BR. Shoulder impact response and injury due to lateral and oblique loading. *Stapp Car Crash J.* 2003;47(35-53).

Brown J, Jing Y, Wang S, Ehrlich P. Patterns of severe injury in pediatric car crash victims: Crash Injury Research Engineering Network database. *J Pediatr Surg.* 2006;41(2):362–367.

Burdi AR, Huelke DF, Snyder RG, Lowrey GH. Infants and children in the adult world of automobile safety design: pediatric and anatomical considerations for design of child restraints. *J. Biomech.* 1969;2:267–280.

Irwin AL, Mertz HJ. Biomechanical basis for the CRABI and Hybrid III child dummie, SAE 973317. Paper presented at: Proc. 41st Stapp Car Crash Conference, Society of Automotive Engineers; 1997; Warrendale, PA.

Irwin AL, Mertz HJ, Elhagediab AM, Moss S, Beach PV. Guidelines for assessing the biofidelity of side impact dummies of various sizes and ages. *Stapp Car Crash J.* 2002;46:297–319.

Lopez-Valdes FJ, Forman J, Kent R, Bostrom O, Segui-Gomez M. A comparison between a child-size PMHS and the Hybrid III 6 YO in a sled frontal impact. *Ann Adv Automot Med.* 2009;53:237–246.

McCray L, Scarboro M, Brewer J. Injuries to children one to three years old in side impact crashes. Paper presented at: 20th International Technical Conference on the Enhanced Safety of Vehicles; June 18-21, 2007; Lyon, France.

Martin P. *Anthropomorphic Test Devices; Q3s 3-Year-Old Child Side Impact Test Dummy, Incorporation of Reference* . Washington, DC; National Highway Traffic Safety Administration, US Department of Transportation; 2013. DOT 202-366-9324.

Melvin JW. Injury assessment reference values for the CRABI 6-month infant dummy in a rear-facing infant restraint with airbag deployment, SAE 950872. Paper presented at: Society of Automotive Engineers International Congress and Exposition; 1995; Warrendale, PA.

Seacrist T, Balasubramanian S, García-España JF, Maltese MR, Arbogast KB, Lopez-Valdes FJ, Kent RW, Tanji H, Higuchi K. Kinematic comparison of pediatric human volunteers and the Hybrid III 6-year-old anthropomorphic test device. *Ann Adv Automot Med.* 2010;54:97–108.

Seacrist T, Samuels M, García-España, Felipe J, Arbogast KB, Mathews EA, Balasubramanian S, Maltese MR, Longhitano D, St. Lawrence S. Kinematic comparison of the Hybrid III and Q-series pediatric ATDs to pediatric volunteers in low-speed frontal crashes. *Ann Adv Automot Med.* 2012;56:285–298.

Seacrist T, Mathews EA, Balasubramaninan S, Maltese M, Arbogast KB. Evaluation of the Hybrid III and Q-Series pediatric ATD upper neck loads as compared to pediatric volunteers in low-speed front crashes. *Ann Biomed Eng.* 2013:41(11):2381-2390.

Seacrist T, Locey C, Mathews E, Jones D, Maltese M, Arbogast K. Evaluation of pediatric ATD biofidelity as compared to child volunteers in low-speed far-side oblique and lateral impacts. *Traffic Inj Prev.* 2014, *Under Review*.

Sherwood CP, Shaw CG, van Rooij L, Kent RW, Gupta PK, Crandall JR, Orzechowski KM, Eichelberger MR, Kallieris D. Prediction of cervical spine injury risk for the 6-year-old child in frontal crashes. *Ann Proc Assoc Adv Automot med.* 2002;46:231–247.

Starnes M, Eigen AM. *Fatalities and injuries to 0-8 year old passenger vehicle occupants based on impact attributes.* Washington, DC; National Highway Traffic Safety Administration, US Department of Transportation; 2002. DOT HS 809 410.

Suntay B, Moorhouse K, Bolte IV J. Characterization of the pediatric shoulder's resistance to lateral loading conditions. Paper presented at: 22nd International Technical Conference on the Enhanced Safety of Vehicles; June 13-16, 2011; Washington, DC.

Thollon L, Cavallero C, Pu M, Brunet PC. The thoracic member under side impact: an experimental approach. *Int J Crashworthiness.* 2001;6(3):307–319.

van Ratingen MR, Twisk D, Schrooten M, Beusenberg MC, Barnes A, Platten G. Biomechanically based design and performance old child crash targets for a 3-year old dummy for frontal and side impact, SAE 973316. Paper presented at: Proc. 2nd Child Occupant Protection Symposium Society of Automotive Engineers; 1997; Warrendale, PA.

Viano DC, Parenteau CS. Fatalities of children 0-7 years old in the second row. *Traffic Inj Prev.* 2008;9(3):231–237.

Wolanin MJ, Mertz HJ, Nyznyk RS, Vincent JH. Description and basis of three-year-old child dummy for evaluating passenger inflatable restraint concepts. Paper presented at: 9th International Conference on Experimental Safety Vehicles; 1982; Kyoto, Japan.